REPORT DOCUMENTATION PAGE

Form Approved
OMB No. 0704-01-0188

PLEASE DO NOT RETURN YOUR FORM TO THE ABOVE ADDRESS.

1. REPORT DATE *(DD-MM-YYYY)*	2. REPORT TYPE	3. DATES COVERED *(From - To)*
28-10-2002	Journal Article	

4. TITLE AND SUBTITLE
Micromachined Fabry–Perot interferometer for motion detection

5a. CONTRACT NUMBER

5b. GRANT NUMBER

5c. PROGRAM ELEMENT NUMBER

6. AUTHORS
Richard L. Waters[a]
Monti E. Aklufi

5d. PROJECT NUMBER

5e. TASK NUMBER

5f. WORK UNIT NUMBER

7. PERFORMING ORGANIZATION NAME(S) AND ADDRESS(ES)
[a]SSC San Diego
53560 Hull St.
San Diego, CA 92152-5001

8. PERFORMING ORGANIZATION REPORT NUMBER

9. SPONSORING/MONITORING AGENCY NAME(S) AND ADDRESS(ES)

10. SPONSOR/MONITOR'S ACRONYM(S)

12. DISTRIBUTION/AVAILABILITY STATEMENT
Approved for public release; distribution is unlimited.

13. SUPPLEMENTARY NOTES

14. ABSTRACT

The monolithic integration of a Fabry–Perot interferometer and a (100) silicon photodiode is reported for use as a highly sensitive transduction method in the detection of minute displacements of a proof mass attached to a spring. The combination results in a compact device with active transistor-like amplification and minimal parasitic elements. The transducer is fabricated using standard surface micromachining techniques. The finesse of the optical cavity, incident optical power, and geometry of the mirror and support structure control the sensitivity of the transducer. A transduction of more than 2285 A/m, percent change in transmission with displacement of 3%/nm, small-signal voltage amplification of 460 V/V output resistance of 100 MΩ and transconductance of 1 mA/V have been obtained thus far for a single device without amplification.

Published in *Applied Physics Letters*, Volume 81, Number 18, October 28, 2002.

15. SUBJECT TERMS
Fabry–Perot interferometer
motion detection
transducer

16. SECURITY CLASSIFICATION OF:			17. LIMITATION OF ABSTRACT	18. NUMBER OF PAGES	19a. NAME OF RESPONSIBLE PERSON
a. REPORT	b. ABSTRACT	c. THIS PAGE			Richard Waters, Code 2876
U	U	U	UU	3	19B. TELEPHONE NUMBER *(Include area code)* (619) 553-6404

Micromachined Fabry–Perot interferometer for motion detection

Richard L. Waters[a] and Monti E. Aklufi
Integrated Circuit Fabrication Facility, 2876, SPAWAR Systems Center, San Diego, California 92152-5001

(Received 14 May 2002; accepted 10 September 2002)

The monolithic integration of a Fabry–Perot interferometer and a (100) silicon photodiode is reported for use as a highly sensitive transduction method in the detection of minute displacements of a proof mass attached to a spring. The combination results in a compact device with active transistor-like amplification and minimal parasitic elements. The transducer is fabricated using standard surface micromachining techniques. The finesse of the optical cavity, incident optical power, and geometry of the mirror and support structure control the sensitivity of the transducer. A transduction of more than 2285 A/m, percent change in transmission with displacement of 3%/nm, small-signal voltage amplification of 460 V/V, output resistance of 100 MΩ and transconductance of 1 mA/V have been obtained thus far for a single device without amplification. © *2002 American Institute of Physics.* [DOI: 10.1063/1.1518557]

Numerous transduction techniques have been investigated for detecting minute displacement of a proof mass attached to a spring for acoustic, vibration, temperature, and inertial sensors. These techniques include the measurement of charge across a variable capacitor,[1,2] change in resistance of a hinge using piezoresistive materials,[3,4] change in optical reflection from a Bragg grating,[5] and change in tunneling current across a well-controlled airgap.[6–9] Of those techniques, tunneling-based transducers offer the best promise for realizing highly sensitive displacement sensors due to the exponential sensitivity of the tunneling phenomena with electrode separation. Currents in a tunnel transducer are usually limited to (1–2) nA due to the small emitting area, usually one atom on the surface of each electrode or the superposition of a small number of atoms with varying separation. Tunneling currents also tend to possess a large flicker noise component especially as the tunneling current increases.[7] In addition, thermal expansion and thermal coefficient mismatches as well as variability in tunneling barrier heights from one device to another have been reported.[8]

In this letter, we report on the monolithic integration of a Fabry–Perot interferometer and a (100) silicon photodiode, in the initial stages of development, that is small, lightweight, and surpasses the raw sensitivity of tunneling-based transducers given in (amps/meter). The reported design is compact and thus has minimal parasitic elements, possesses transistor-like characteristics for use as an active pickoff, and can be arrayed to increase the sensitivity/frequency range or decrease the noise floor of the composite system. The fabrication and structure of the Fabry–Perot/photodetector combination is similar to those reported for Fabry–Perot cavities incorporated with III–V light emitting diodes.[10–13]

A Fabry–Perot interferometer is an extremely sensitive optical device typically used to measure the fine spectral nature of materials with sub-Angstrom wavelength resolution. A Fabry–Perot interferometer is comprised of two optically flat, parallel, semitransmissive mirrors separated by some distance, y. The same sensitivity used for wavelength resolution can be used to detect motion of one mirror with respect to a second reference mirror when monochromatic light is incident normal to the surface of the resonant cavity. For the case where both mirrors are identical, and no absorption occurs within the mirrors or the medium separating the mirrors, an expression for the photogenerated current within the diode can be written as

$$I_{\mathrm{ph}} = \Re P_{\mathrm{in}} A \frac{1}{1 + F \sin^2\left[\frac{2\pi}{\lambda}[n_1 y(a) + n_{\mathrm{ox}} d_{\mathrm{ox}}]\right]}, \tag{1}$$

where $\Re$ is the responsivity of the photodiode in A/W, P_{in} is the incident optical power density normal to the surface of the resonant cavity, A is the area of the photodiode, F is the finesse of the optical cavity and is related to the reflectivity of the mirrors, λ is the incident wavelength, n_1 and $y(a)$ are the index of refraction and acceleration dependent air-gap of the medium between the mirrors, and n_{ox} and d_{ox} are the index of refraction and thickness of the upper mirror. In the derivation of Eq. (1), the upper mirror was assumed to be a uniform silicon dioxide membrane. By taking the derivative of the photogenerated current, Eq. (1), with respect to input acceleration and rewriting the result in terms of I_{ph}, Eq. (2) obtains:

$$\frac{dI_{\mathrm{ph}}}{da} \propto \frac{I_{\mathrm{ph}}^2 F}{\Re P_{\mathrm{in}} \omega_0^2}, \tag{2}$$

where ω_0 is the resonant frequency of the mechanical structure and is related to the ratio of upper mirror mass and effective spring constant. The sensitivity of the photogenerated current to changes in input acceleration is dependent upon the photogenerated current, I_{ph}, finesse of the cavity, and resonant frequency. Increasing either the input power or finesse of the cavity or decreasing the resonant frequency will increase the acceleration sensitivity of this transducer. For a nonideal mirror that may have a finite thickness and absorption, a characteristic matrix, similar to that obtained for a transmission line structure, needs to be solved for each layer comprising the mirror. Equations (1) and (2) are ap-

[a]Electronic mail: watersrl@spawar.navy.mil

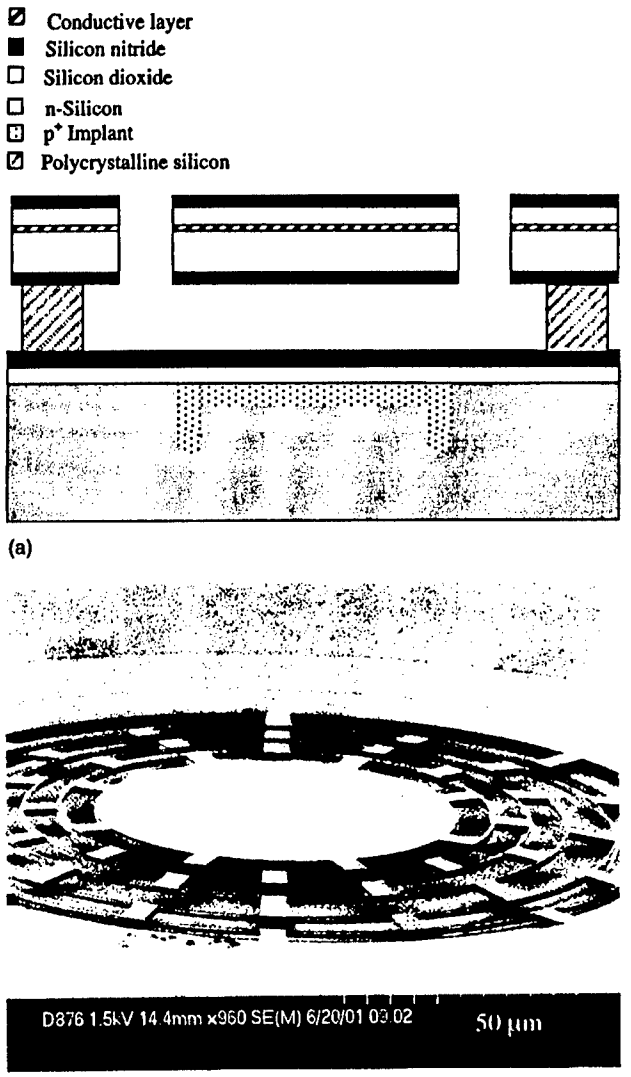

FIG. 1. (a) Is a cross-sectional drawing of the transducer; (b) is a SEM micrograph of an example sensor structure.

proximations and meant only to give a tractable expression and insight into the behavior of this transducer.

The sensors were fabricated using surface micromachining techniques at the Space and Naval Warfare Systems Center (SPAWAR SYSCEN), San Diego's Integrated Circuit Fabrication Facility (ICFF). Phosphorus-doped (100) bulk silicon with a resistivity of $\rho = 10-30\ \Omega$ cm served as the starting material. Boron implantation was performed to form a shallow one-sided junction so to collect as much transmitted light into the depletion region of the photodiode as possible thus increasing the responsivity, $\Re$, (A/W). A series of well-controlled silicon dioxide and silicon nitride depositions, in combination with dry/wet etching, were used to form the dielectric upper and lower mirrors of the final structure shown in Fig. 1(a). A thin semitransparent conductive layer was incorporated into the upper mirror to allow for electrostatic control of the air-gap spacing between the upper and lower mirrors. The sacrificial layer between the upper and lower mirrors was 0.8 μm of undoped polycrystalline silicon that was later removed using a highly selective anisotropic tetra-methyl ammonium hydroxide etch with silicic

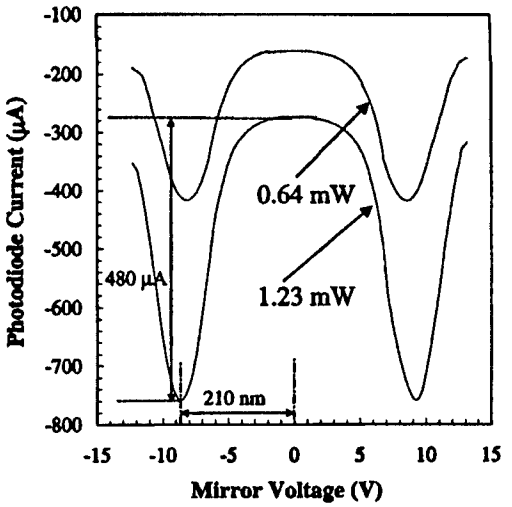

FIG. 2. Photogenerated current as a function of the applied voltage (force) between the mirrors using two different input power densities of 625 and 325 kW/m^2, photodiode diameter of 50 μm, and measured responsivity of 0.65 A/W. As the optical power increases so too does the maximum slope and hence displacement sensitivity. From the figure, a lower bound for the maximum transduction of 2285 A/m was obtained along with a displacement sensitivity of 3%/nm.

acid at 80 °C. Figure 1(b) is a SEM micrograph detailing the structure of the upper mirror as well as an example spring geometry. In total, more than 140 accelerometers with unique spring designs were fabricated on a 9 mm×9 mm die. The polycrystalline silicon support structure/pedestal, shown in Fig. 1(a), is not viewable in the SEM micrograph of Fig. 1(b).

The final sensor includes three contacts corresponding to the upper mirror, photodiode anode, and photodiode cathode. The anode acts as the lower mirror electrode. Potentials applied between the upper mirror and anode results in an electrostatic force that can be used to control the air-gap separation in a force rebalance mode and to modulate the photocurrent for use as an active optical element.

Electro-optical measurements were taken using an HP4156B parameter analyzer in conjunction with a Sanyo DL830 semiconductor laser operating at a center wavelength of approximately 830 nm and a maximum output power of 150 mW. Typical measured dark current of the photodiodes was 1 pA at -1 V and 10 pA at -60 V with an output resistance greater than 100 MΩ. Figure 2 is a plot of the photogenerated current as a function of the applied electrostatic force between the upper and lower mirrors for two different optical power densities, 325 and 625 kW/m^2, respectively, incident on a sensor with a 50 μm diameter diode. It can be observed that in the absence of detector saturation, an increase in optical power causes a corresponding linear increase in differential gain consistent with Eq. (2). It should also be noted that the maximum transduction, i.e., maximum slope in Fig. 2, could not be extracted due to feedback from the n-type substrate affecting the ideal voltage-displacement calculations. Instead, a lower bound for transduction was measured by taking the change in photocurrent of 480 μA between a maximum and a minimum transmission peak and dividing by the corresponding change in displacement of $\lambda/4$ or 210 nm resulting in a lower limit transduction of 2285 A/m. This represents a high transduction factor for a MEMS-

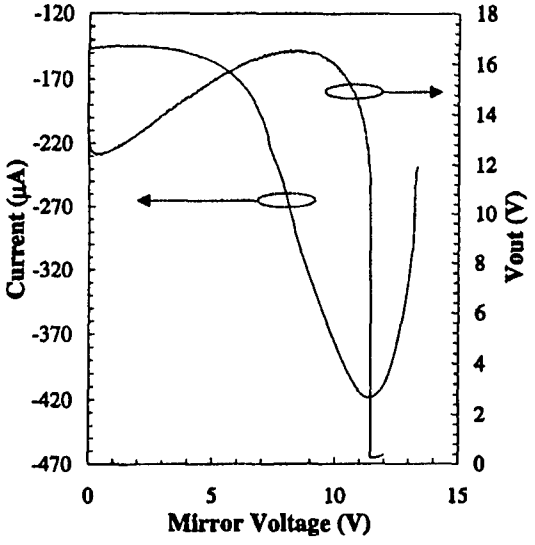

FIG. 3. Output voltage vs input voltage applied as measured across the mirrors using a current source of $-420\ \mu$A as the load. Due to the transistor action of the sensor and high output resistance of the photodiode, large voltage gains can be achieved.

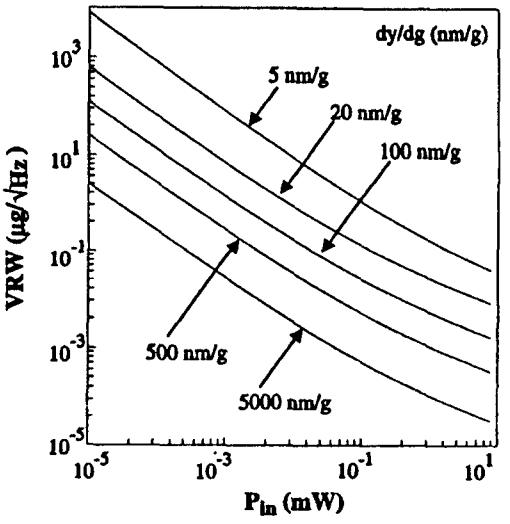

FIG. 4. Plot of velocity random walk (VRW) vs the input optical power for several displacement sensitivities dy/dg in units of (nm/g). The curves were calculated using $T=300$ K, $R_p=1$ kΩ, $\Re=0.67$ A/W, $A=7.85\times10^{-9}$ m^2, and a value of 2%/nm for the change in transmission with displacement.

based motion detector without the use of amplification circuitry and is more than 2 orders of magnitude larger than the 9.4 A/m reported for tunneling based transducers.[12] The percent change from maximum transmission per nanometer of displacement can be calculated from Fig. 2 to be 3%/nm. The maximum transconductance as measured from Fig. 2 is 1 mA/V.

Theory, as outlined in Eqs. (1) and (2), suggests that the transduction of 2285 A/m can be increased further. Assuming a finesse of 10, a responsivity of 0.67 A/W at 830 nm, a photodiode radius of 50 μm, an input optical power density of 500 kW/m^2 corresponding to 4 mW of incident optical power and differential transmission of 2%/nm results in a sensitivity of 5360 A/m. This value can be increased by increasing the reflectivity of the mirrors through the deposition of additional dielectric stacks thereby increasing the finesse, increasing the photodiode radius or by increasing the input optical power to the point of saturating the photodetector.

To extract the small-signal amplification of the sensor, a current sink of 420 μA was applied to the sensor as a load. Figure 3 is a plot of the measured voltage across the photodiode, y-2 axis, versus the input voltage across the mirrors. The maximum measured small-signal amplification on this device was 460 V/V with further amplification being limited by the input voltage resolution of the HP4156B parameter analyzer.

The sensitivity of the sensor can be calculated by examining the noise sources present within the sensor. In the absence of Brownian motion, i.e., a vacuum, shot noise of the photodetector/laser combination and resistive noises are dominant. The laser will also exhibit an additional random induced noise (RIN) but it is expected that for sufficient values of photogenerated current the shot noise of the photodetector will dominate and swamp out the laser RIN. The resistive noise is constant given a fixed temperature and determined by the value of the load resistor attached to the sensor when operated as an inverting amplifier. Meanwhile, the shot noise increases with the square root of the input optical power. The velocity random walk (VRW), a figure of merit for accelerometers, is given in Eq. (3) as the reciprocal of the signal to noise ratio (SNR) which includes both the resistive and shot noise contributions:

$$\mathrm{VRW}=\frac{\sqrt{4k_BTR_p}+\sqrt{2qP_{in}A\Re R_p}}{2\left(P_{in}A\Re\frac{dy}{dg}\frac{dT_r}{dy}\right)R_p}, \tag{3}$$

where k_B is Boltzmann's constant, T is the temperature, g is input acceleration normal to the surface of the mirror ($1g=9.8$ m/s^2), A is the area of the photodiode, R_p is the load resistance, dT_r/dy is the change in transmission with mirror spacing and is approximately equal to 2%/nm for a finesse of 10, and dy/dg is the mechanical sensitivity of the sensor given in (nm/g). Figure 4 shows the velocity random walk (VRW) as a function of the input optical power for various displacement sensitivities given in (nm/g). Figure 4 was generated assuming a temperature, T, of 300 K, a photodiode diameter of 100 μm, a load resistor value, R_p, of 1 kΩ and a responsivity, $\Re$, of 0.67 A/W at a wavelength of 830 nm. The displacement sensitivity, dy/dg, given in (nm/g) is determined by the geometrical structure, mass and spring constant, all of which can be adjusted for a particular application. For example, a resonant frequency of 500 Hz results in a displacement sensitivity of $\sim$100 nm/g ($9.83/\omega_o^2$), and according to Fig. 4, a corresponding VRW of 80 ng/√Hz at an input power level of 100 μW.

In conclusion, we reported on the initial development of a three-terminal electro-optical transducer possessing transistor-like characteristics based upon the monolithic integration of a Fabry–Perot interferometer and a photodiode on a (100) silicon substrate. The transduction mechanism was shown to have raw sensitivity greater than 2000 A/m. Initial experimental electro-optical measurements were shown demonstrating the viability of this transduction mechanism in realizing high sensitivity motion detectors.